EUROPEAN JOURNAL OF BIOMEDICAL AND PHARMACEUTICAL SCIENCES
http://www.ejbps.com

ISSN 2349-8870
Volume: 12
Issue: 5
Year: 2025

DESIGN, DEVELOPMENT AND CHARACTERIZATION OF NANOSTRUCTURED LIPID CARRIERS LOADED WITH PROGUANIL.

Indrayani S. Pagare*[1], Utkarsh R. Mandage[2], Ashwini I. Patil[3] and Jagruti R. Patil[4]

[1]Department of QA, Ravindra Vidya Prasarak Mandal Institute of Pharmacy, Dwarka, Nashik, India.
[2]Department of Pharmacognosy, Ravindra Vidya Prasarak Mandal Institute of Pharmacy, Dwarka, Nashik, India.
[3]Department of Pharmaceutics, TSPM's Trimurti Institute of Pharmacy Paldhi Bk, India.
[4]Department of Pharmaceutics, St. Wilfred Institute of Pharmacy, Mira road, Mumbai.

***Corresponding Author: Indrayani S. Pagare**
Department of QA, Ravindra Vidya Prasarak Mandal Institute of Pharmacy, Dwarka, Nashik, India.

Article Received on 18/03/2025 **Article Revised on 08/04/2025** **Article Published on 28/04/2025**

ABSTRACT
Nanotechnology and nano-science hold significant promise for advancing various research fields and applications, attracting substantial investments globally. However, their implementation raises safety, regulatory, and ethical challenges. Nano-materials' unique properties, such as increased surface area and quantum effects, enhance reactivity, strength, electrical characteristics, and in vivo behavior. Nanoparticles, defined as particles sized 10-1000 nm, play a crucial role in drug delivery systems by improving oral uptake efficiency, patient compliance, and market expansion for injectable drugs. Colloidal drug carriers, including liposomes, micelles, and polymeric nanoparticles, enhance drug specificity, bioavailability, and protection against enzymatic degradation. These carriers also facilitate drug passage across the blood-brain barrier. Ideal carrier systems should be non-toxic, possess high drug-loading capacity, provide controlled release, and be economically scalable. Nanometric colloidal carriers include lipidic flexible particles, nanoemulsions, nanosuspensions, polymeric nanoparticles, solid lipid nanoparticles, and nanostructured lipid carriers, each offering unique advantages in drug delivery.

INDEXTERMS: Nanoemulsion, Nanosuspension, Lipid carrier.

INTRODUCTION
Nanotechnology and nanoscience are widely recognized for their significant potential to benefit many areas of research and application. They are attracting increasing investments from governments and private sector businesses worldwide. Concurrently, the application of nanoscience raises new challenges in safety, regulatory, and ethical domains, necessitating extensive debates on all levels. The prefix "nano" is derived from the Greek word for dwarf. Nanomaterials differ significantly from other materials due to two major principal factors: increased surface area and quantum effects. These factors can enhance properties such as reactivity, strength, electrical characteristics, and in vivo behavior. As the particle size decreases, a greater proportion of atoms are found at the surface compared to inside. For example, a particle size of 30 nm has 5% of its atoms on the surface, at 10 nm 20%, and at 3 nm 50% of the atoms are on the surface (Thassu et al., 2017).

Nanoparticles are defined as particulate dispersions or solid particles with a size in the range of 10-1000 nm. The drug can be dissolved, entrapped, encapsulated, or attached to a nanoparticle matrix (Mohanraj and Chen, 2016). The dimensions of nanotechnology are shown in Fig. 1.1.

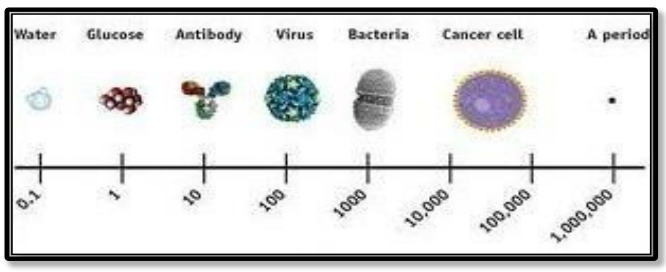

[**Dimensions of nanotechnology](Fig1.1).**

Carrier systems that facilitate intestinal uptake of new molecules are of major interest in the drug delivery arena. Drug delivery systems that provide a route of administration not involving injection can improve patient compliance and expand the market for existing injectable drugs. The factors important for the oral efficiency of a vehicle system include small particle size, appropriate surface properties, mucoadhesive and targeting moieties, stability, and dosage, all of which are major factors influencing the efficiency of oral uptake (Zarif, 2006).

1.2 Colloidal Drug Carriers

New technologies employed in drug discovery have led to the finding of many powerful substances. The development of new drugs alone is not sufficient to ensure progress in drug therapy. Poor water solubility and insufficient bioavailability of new drug molecules are common problems in modern drug therapy. Therefore, there is an increasing need to develop a drug carrier system that overcomes these drawbacks combined with optimal drug release (Hommoss, 2018). The aim of using colloidal carriers is generally to increase specificity towards cells or tissues, improve the bioavailability of drugs by increasing their diffusion through biological membranes, and/or protect them against enzyme inactivation. Moreover, colloidal systems allow access across the BBB (blood-brain barrier) of non-transportable drugs by masking their physico-chemical characteristics through their encapsulation (Garcia et al., 2015).

Among particulate drug carriers, liposomes, micelles, and polymeric nanoparticles are the most extensively studied and possess the most suitable characteristics for encapsulating many drugs and diagnostic (imaging) agents. Many other systems meeting specific requirements (reviewed in this book) are also suggested and currently under development. Making these nanocarriers multifunctional and stimuli-responsive can dramatically enhance the efficiency of various drugs carried by these carriers. These functionalities are expected to provide: (a) prolonged circulation in the blood, (b) the ability to specifically recognize and bind target tissues or cells via surface-attached specific ligands, (c) the ability to respond to local stimuli characteristic of the pathological site, and (d) the ability to penetrate inside cells bypassing lysosomal degradation for efficient targeting of intracellular drug targets (Torchilin, 2006).

This carrier system should have no toxicity (acute and chronic), have sufficient drug loading capacity, and possess drug targeting and controlled release characteristics. It should also provide chemical and physical stability for the incorporated drug. The feasibility of production scaling up with reasonable overall costs should be available (Barratt, 2010; Mehnert and Mader, 2011; Mainardes and Silva, 2014).

Drug Delivery Approaches Based on Nanometric Colloidal Carriers

Nanometric colloidal carriers are listed below

- Lipidic flexible particles such as liposomes, niosomes, ethosomes, and transferosomes
- Nanoemulsions and nanosuspensions
- Polymeric nanoparticles (Polymeric NP)
- Solid lipid nanoparticles (SLN) and nanostructured lipid carriers (NLC)

MATERIAL AND METHODS

Table no. 1: The list of material and instrument with their manufacturer which is used in experiment.

Sr.No	Particulars	Manufacturer/ Suppliers
Drug		
01	Proguanil	Glenmark Mumbai, India. (Batch No. PRG/1569B/0190)
Excipient		
01	Compritol 888 PRG	Gattefosse (France)
02	Oleic Acid	Loba chemie, Mumbai, India.
03	Pluronic F-68	HIMedia Lab. Pvt. Ltd, Mumbai, India.
04	Soya lecithin	PHOSPHOLIPID GmbH, Germany.
Chemicals & Reagents		
01	KH_2PO_4	Qualigens fine chemicals, Navi Mumbai, India
02	KCl	Qualigens fine chemicals, Navi Mumbai, India
03	NaoH	Loba Chemie Pvt. Ltd; Mumbai, India
04	Methanol	Merck Specialities Pvt. Ltd., Worli, Mumbai, India
05	Acetonitrile	Merck Specialities Pvt. Ltd., Worli, Mumbai, India
06	Ethanol	Merck Specialities Pvt. Ltd., Worli, Mumbai, India

07	HCl	Rankem, RFCL, Ankleshwar, Gujarat, India
Equipment's		
01	Electronic balance	AUX 120, Shimadzu, Japan
02	Ultraviolet Spectrophotometer	Shimadzu 1700, Japan
03	Melting point apparatus	Thermocal, Analab Sci. Instru., Vadodara, India
04	SonicPRGr	LAB-HOSP, Mumbai
05	Orbital shaking incubPRGr	CIS-24, Remi instruments Ltd., Mumbai, India
06	Digital pH meter	Elico Model- LI 612
07	Dissolution test apparatus	Electrolab, TDT 08 L dissolution tester USP
08	Differential scanning calorimeter	METTLER DSC 30 S, Mettler Toledo
09	KBR press	KBR press, TSI, Mumbai
10	Infra-Red Spectrophotometer	8400S, Shimadzu, Kyoto Japan.
11	Scanning electron microscope	JSM, 6390, USA
12	Stability chamber	CHM-10S Remi Lab, Mumbai
13	HPLC	Agilent 1200 Series
14	Ultracentrifuge	Optima max XP, Beckman coulter, USA
15	Zetasizer	Nano ZS90, Malvern ltd., UK
16	High pressure homogenizer	PANDA 2K, Niro Soavi, Italy
17	Water bath	Equitron

(All the chemicals used were of analytical reagent grade)

Preformulation study

Preformulation study is one of the important pre-requisite in development of any drug delivery system. It gives the information needed to define the nature of the drug substance and provide a framework for the drug combination with pharmaceutical excipients in the dosage form. Hence, Preformulation studies on the obtained sample of drug are required.

Confirmation of drug

Confirmation of drug was carried out by Melting point determination, Infrared spectroscopy (IR) and DSC.

Melting point method

Melting point determination is prime confirmation of drug. In this method, drug whose analysis to be carried out was filled into capillary tube and tied to the thermometer in such a way that it remains dipped in liquid paraffin bath. The temperature range at which the drug starts melting and complete melting was noted.

Infrared Spectroscopy

IR spectrum of drug was measured in the solid state as potassium bromide (KBr) mixture. The pure PRG was previously ground and mixed thoroughly with KBr, an infrared transparent matrix at 1:100 (sample: KBr) ratio, respectively. The KBr pellets were prepared by applying 10-12 metric ton of pressure in a motorized pellet press (Kimaya engineers, India). The pellets were then scanned over a wave range of 4000 – 400 cm^{-1} and spectra was obtained by using a FTIR spectrometer- 430 (Shimadzu 8400S, Japan).

Differential Scanning Calorimetry

Melting point of drug was determined by using Differential Scanning Calorimetry. Thermogram for PRG was obtained using DSC (Mettler DSC 1 star system, Mettler- Toledo, Switzerland). The drug was sealed in perforated aluminum pan and heated at constant rate of 10°C/min over the temperature ranges of 30-300°C.

Drug -Excipients Interaction Study

The drug-excipients interaction study was carried out using FTIR and DSC.

Fourier Transform-Infrared spectroscopy (FTIR)

FTIR spectra of PRG, Compritol 888 PRG, oleic acid and physical mixture of lipids with PRG were studied. Above samples were mixed with KBr of IR grade in the ratio of 1:100 and compressed using motorized pellet press (Kimaya Engineers, India) at 10-12 tones pressure. The pellets were then scanned using FTIR spectrophotometer (Shimadzu 8400S, Japan). The FTIR spectra of mixtures were compared with that of the FTIR Spectra of pure drug and lipid, to confirm any changes occur or not in the principle peaks of spectra of plain drug and lipid.

Differential Scanning Calorimetry Study

Thermal analysis was carried out for PRG, Compritol 888 PRG and physical mixture of them were conducted using DSC (Mettler DSC 1 star system, Mettler-Toledo, Switzerland) at a heating rate of 10°C/min. The measurements were performed at a heating range of 40 to 300°C under nitrogen atmospheres.

STANDARD CALIBRATION CURVES

Standard calibration curve in Methanol

Accurately weighed 10 mg of PRG was dissolved in 100 mL of methanol to obtain working standard solution of 100 µg/mL. Aliquots of 0.3 mL, 0.6 mL up to 1.8 mL from the stock solution representing 3, 6 up to 18 µg/mL of drug were transferred to 10 mL volumetric flask and the volume was adjusted up to mark with methanol. Absorbances of the above solutions were taken at 251 nm against the blank solution that is methanol without drug. A graph of absorbance vs. concentration was plotted.

Standard calibration curve in pH 1.2 buffer system

Accurately weighed 10 mg of PRG was dissolved in 100 mL of pH 1.2 buffer solutions to obtain working standard solution of 100 µg/mL. Aliquots of 1.5 mL, 3 mL up to 9 mL from the stock solution representing 15, 30 up to 90 µg/mL of drug were transferred to 10 mL volumetric flask and the volume was adjusted to mark with same blank solution. Absorbance of the above solutions were taken at 251 nm against the blank solution prepared in the same manner without adding the drug. A graph of absorbance vs. concentration was plotted.

Calibration Curve in pH 6.8 Phosphate Buffer

Ten mg of PRG was dissolved in 100 mL of pH 6.8 buffer to obtained working standard of 100 µg/mL. Aliquots of 0.5 mL, 1 mL up to 3.5 mL from the stock solution representing 5 to 35 µg/mL of drug were transferred to 10 mL volumetric flask and the volume was adjusted to mark with pH 6.8 buffer. Absorbances of the above solution were taken at λ_{max} 251 nm against the blank solution prepared in the same manner without adding the drug.

Calibration Curve in pH 7.4 Phosphate Buffer

10 mg of PRG was dissolved in 100 mL of pH 7.4 buffer to obtained working standard of 100 µg/mL. Aliquots of 0.2 mL, 0.4 mL up to 1.4 mL from the stock solution representing 2 to 14 µg/mL of drug were transferred to 10 mL volumetric flask and the volume was adjusted to mark with pH 7.4 buffers. Absorbances of the above solution were taken at λ_{max} 251 nm against the blank solution prepared in the same manner without adding the drug.

Solubility determination of PRG

An excess amount of PRG was added to each of distilled water, methanol, pH 1.2 and phosphate buffer (6.8 and 7.4). The mixtures were then kept at ambient temperature for 72 h in an Orbital shaking incubPRGr (CIS-24, Remi instruments Ltd., Mumbai, India) to get equilibrium. The equilibrated samples were centrifuged at 3000 rpm for 5 min (Optima max XP, Beckman coulter, USA). Aliquot portions of the supernatants were taken and properly diluted with phosphate buffer for quantification of PRG spectrophotometrically at 251 nm (Shimadzu 1700, Japan) **(Mokhtar et al., 2008)**.

FORMULATION AND DEVELOPMENT

Partitioning Nature of PRG between the Lipids

Five milligram of PRG was dispersed in a of melted lipid (1 g) added slowly increment of 5 mg for solid lipid and liquid lipid (5 mL) in which 5 mg increment into the liquid lipid then shaken for 30 min, incorporating a mechanical shaker using a hot water bath maintained 10□C above the melting point of the lipid under investigation. The aqueous phase of the above mixture was separated from the lipid by centrifugation at 25000 rpm for 20 min in a high speed centrifuge. The clear supernatant obtained after centrifugation was suitably diluted with same solvent and analyzed by HPLC (Agilent 1200 Series) at 251 nm □max for PRG content to study its partitioning behaviour with various lipids **(Chalikwar et al., 2012;Venkateswarlu and Manjunath 2004)**.

Formulation Ingredients

Selection of the components for Nanostructured lipid carrier system was based on PRG solubilizing capacity of the excipients and stability of the formulation. The selected components were as follows:

Lipid phase

Solid lipid: Compritol 888 PRG
Oil phase: Oleic Acid

Surfactant phase

Surfactant phase: Pluronic F-68 (Poloxamer 188)
Stabilizer: soya lecithin

Aqueous phase

Double distilled water.

Preparation of PRG loaded NLCs

PRG-NLCs were prepared using high pressure homogenization method. COMP and OA concentration at different levels **(Table 6.1)** and 15 mg of drug utilized. Drug was dissolved in the melted lipid phases which were kept in a heating water bath at 85 ± 0.5°C. The aqueous phase comprised of surfactant and co-surfactant dissolved in water. Both the phases were maintained at a temperature above the melting point of the lipid (85°C). At this temperature, the melted hot lipid phase was then dispersed in the hot surfactant phase, obtaining a pre-emulsion under mechanical stirring (Remi Instruments Ltd., Mumbai, India) at 800 rpm at for 10 mins. Then this warm pre-emulsion was introduced into a high pressure homogenizer (PANDA 2K, Niro Soavi, Italy) at 800 bar pressure and 5 cycles to form the NLC dispersion. Then the NLCs so formulated were allowed to cool at room temperature which was further used for characterization **(Chalikwar et al., 2012)**.

Table 2: The coded and actual values of the variables used in CCRD-RSM of PRG-NLCs preparation.

Independent Variables	Actual values			
	Low (-1)	High (+1)	-alpha	+alpha
X_1= = Total lipid concentration in gm	2	2.5	1.82955	2.67045
X_2= Liquid lipid to total lipid concentration in %	20	40	13.1821	46.8179
X_3= (Soya lecithin) co surfactant concentration in %	40	60	33.1821	66.8179

6.2 Experimental design using Design Expert Software

To design the formulation of lipid based nanoparticles i.e. NLCs, it was essential to recognize the parameters in the formulation as these variables can affect the properties of desired formulation. By identifying the factors that may affect the outcome of experiment and responses that give a measure of the outcome was investigated. In this study the most popular response surface methodology (i.e., CCD) was used to determine the optimum levels of these variables. CCD generally also called Box-Wilson Central composite design. Independent variables include total lipid concentration (X_1), liquid lipid to total lipid concentration (X_2) and co-surfactant concentration (X_3). Were studied at five different concentrations coded as –α, -1, 0, 1, and + α. The value for alpha is calculated to fulfill both rotatability and orthogonality in the design. All independent variables, their levels along with actual and coded values of these variables are shown in **(Table 4)**. Whereas particle size of NLCs (Y_1), zeta potential (Y_2) and drug entrapment efficiency (Y_3) were selected as response parameter as the dependent variables. According to the central composite design matrix generated by Design-Expert software, a total number of 20 experiments, including 8 factorial points, 6 axial points, and 6 replicates at the center point for estimation of pure error sum of squares, were performed **(Table 5)**. Using this design, we were able to choose the best model among the linear, two-factor interaction model and quadratic model due to the analysis of variance (ANOVA) F-value. Design- Expert software was employed for statistical analysis and graph plotting. The effect of independent variables on the responses was calculated by ANOVA through Fisher's test. The *P*-value less than 0.05 were considered to be statistically significant. Evaluation of multiple correlation coefficients (R^2) and adjusted R^2 were employed for best suitability of model. Contour and three-dimensional surface plots were used to reveal the relationship and interaction between the coded variables and the responses. For optimization, the particle size is in its minimum and entrapment efficiency (%) at maximum levels **(Varshosaz et al., 2009, Zhang et al., 2010, Chalikwar et al., 2012 and Zhang et al., 2013).**

Table 3: Formulations of nanostructured lipid carriers loaded with PRG by central composite design.

Run	X_1 (mg)	X_2 (mg)	X_3 (%)
F1	2.25	30	50
F2	2.25	30	50
F3	2	40	40
F4	2.67	30	50
F5	2.5	20	60
F6	2.5	40	40
F7	2	20	40
F8	2.25	30	66.82
F9	2.25	30	50
F10	2	20	60
F11	2.25	30	50
F12	2.5	40	60
F13	2	40	60
F14	2.25	30	50
F15	2.25	13.18	50
F16	2.5	20	40
F17	2.25	30	50
F18	2.25	30	33.18
F19	2.25	46.82	50
F20	1.83	30	50

X_1 = Total lipid concentration in gm (high level-2.5, low level-2), X_2 = Liquid lipid to total lipid concentration in % (high level-40, low level-20), X_3 = Surfactant and co- surfactant concentration in % (high level-60, low level-40)

CHARACTERIZATION AND EVALUATION OF NLCs DISPERSION

Determination of particle size and PDI of the PRG-NLCs

The mean particle size (MPS) analysis of NLCs was performed by photon correlation spectroscopy (PCS) using Zetasizer (Nano ZS 90, Malvern Instruments, UK) at a fixed angle of 90□ at 25□C temperatures. The NLCs dispersion was diluted with distilled water before analysis to get optimum 50-200 kilo counts per seconds (kcps) for measurement. The PCS yielded the mean diameter of the main population and polydispersity index (PI) as a measure for the width of the particle size distribution **(Souto et al., 2004)**.

Zeta potential of the PRG-NLCs

Zeta potential measurements were run at 25□C with electric field strength of 23 V/m, using Zetasizer (Nano ZS 90, Malvern Instruments, UK) **(Chalikwar et al., 2013)**. To determine the zeta potential, samples of PRG-

NLCs were diluted and placed in electrophoretic cell. The zeta potential was calculated as described by Helmholtz– Smoluchowski equation **(Serpe et al., 2004)**.

Determination of entrapment efficiency (EE %) and Drug loading (DL %) of the PRG-NLCs

EE % was calculated by determining the amount of non-encapsulated PRG in aqueous surfactant solution. The drug-loaded NLC dispersion centrifuge and aqueous medium was separated by using Ultracentrifuge (Optima max XP, Beckman coulter, USA). Quantity sufficient volume of PRG-NLCs dispersion was placed in thin wall polyallomer tubes and centrifuge at 15,000 rpm speed for 30 min at 4□C. the concentration of PRG in the aqueous phase was determined using UV–visible spectrophotometer (UV 1700, Shimadzu, Japan) at □max 251 nm. Values of EE % and DL % were calculated using **Eqs. (1)** and **Eqs. (2)** Respectively **(Sanad et al., 2010, Chalikwar et al., 2012)**.

$$EE\ \% = \frac{\text{Amount of drug added} - \text{Amount of drug in supernatant}}{\text{Amount of drug added}} \times 100 \quad (1)$$

$$DL\ \% = \frac{\text{Amount of drug added} - \text{Amount of drug in supernatant}}{\text{Amount of lipid added}} \times 100 \quad (2)$$

***In vitro* release studies of PRG-NLCs**

It is usually known that the release of the drug from nanocarriers is influenced by the various factors such as, structure and composition of the Nano lipid carriers. Hence, the *in vitro* releases of PRG from NLCs were studied.

In vitro release of drug from PRG-NLCs was evaluated in phosphate buffer saline solution (PBS) (pH 6.8), using a dialysis bag diffusion technique. Dialysis membrane with a pore size of 2.4 nm and molecular weight cut off between 100 kDa was used. The dialysis bags were hydrated in phosphate-buffered saline, pH 6.8 overnight before the experiment. NLCs containing PRG were placed in dialysis bags. The dialysis bags were tied at both ends and were placed in the beaker containing 250 mL phosphate buffer saline pH 6.8. The beaker were maintained at 37±2□C and stirred at a constant speed of 100 rpm. At regular intervals of 1, 3, 6, 12, 24, 36, 48, 60, 72, 84 h intervals up to 96 h, 5 ml of dissolution medium was removed and was replaced with the fresh buffer at same temperature to maintained sink condition. The amount of PRG in the aliquots was analyzed by UV-Visible spectrophotometer (UV 1700, Shimadzu, Japan) at □max 251 nm **(Liu et al., 2011, Ekambaram and Sathali A., 2011 and Joshi et al., 2008)**.

max XP, Beckman coulter, USA) plasma was collected and stored at -20□C until analysis. The concentration PRG in rat plasma analyzed by Kinetica 5 and HPLC (Agilent 1200 Series) at □max 251 nm **(Chalikwar et al., 2012, Zhuang et al., 2010, Calvo et al., 2011 and Chen et al., 2010)**.

OPTIMIZATION DATA ANALYSIS

For optimization data analysis, the design matrix used was built by the statistical software package, Design-Expert (version 8.0.0; Stat-Ease, Inc., Minneapolis, Minnesota, USA)

SOLID STATE CHARCTERISATION

Lyophilization of NLCs

The PRG-NLCs aqueous dispersion with 3 % cryoprotectant (Mannitol) was frozen in a refrigerPRGr at –75°C for 24 h. Then the samples were lyophilized using a lab freeze- dryer (VirTis Benchtop K, SP scientific, Warminster USA). The freeze-drying was conducted for 72 h. After this, the vials were sealed with rubber caps **(Abdelwahed et al., 2006, Jain et al., 2013)**.

Scanning electron microscopy (SEM)

Surface morphology of the NLC studied out by scanning electron microscope. The optimized formulation was kept onto metal plate and dried under vacuum to form a dry film which was then observed under the scanning electron microscope (LEO 440i; Leo Electron Microscopy Ltd., Cambridge, UK) **(Tan et al., 2010)**.

X-Ray Diffraction (XRD)

Crystalline structures of the NLCs were investigated using X-ray diffractometer (Bruker AXS D8 Advance, Germany). The samples were mounted on a sample holder and XRD patterns were scanned in the range of 3–80□ at a chart speed of 5□ per min. Samples used for measurement were pure PRG, physical mixture of drug and COMP, and drug-loaded lyophilized NLC formulation **(Chalikwar et al., 2013, Liu et al., 2011, Zhuang et al., 2010, Lin et al., 2007 and Almeida et al., 2012)**.

Stability studies of PRG-NLCs

The physical stability of PRG-NLCs was determined according to **(Chalikwar et al. 2012)**. The lyophilized powder sample of final optimized formulation was utilized for carrying out accelerated stability study according to International Conference on Harmonisation (ICH) Q1A (R2) guidelines. Drug products intended for storage in a refrigerPRGr ICH guidelines suggested long term stability at 5°C ± 3°C and Accelerated stability at 25°C ± 2°C/60 % RH ± 5% RH for Minimum time period. Accelerated stability study was performed with the principal aim to assess the stability of NLCs at 25°C ± 2°C/60 % RH ± 5 % RH with respect to particle size, PDI and EE **(Kalam et al., 2010 and Chalikwar et al., 2012)**.

RESULTS AND DISCUSSION

PREFORMULATION STUDY

Confirmation of drug

Confirmation of drug was carried out by simple melting point determination, infrared spectroscopy and differential scanning calorimetry (DSC).

Melting point method

The melting point of PRG was confirmed by capillary method using melting point apparatus (Thermocal,

Analab Sci. Instru., and Vadodara, India). The melting point of PRG was found to be in the range of 127-130□C. The observed melting point of PRG was confirmed with the standard melting point of PRG i.e. 127 - 230□C.

Infrared Spectroscopy

The IR spectrum was measured in the solid state as potassium bromide mixture. The IR spectrum of PRG is displayed in **Fig 7.1**. Principal peaks and chemical group present in IR spectra of PRG is presented in **Table (Hardikar et al., 2013; Nair et al., 2012).**

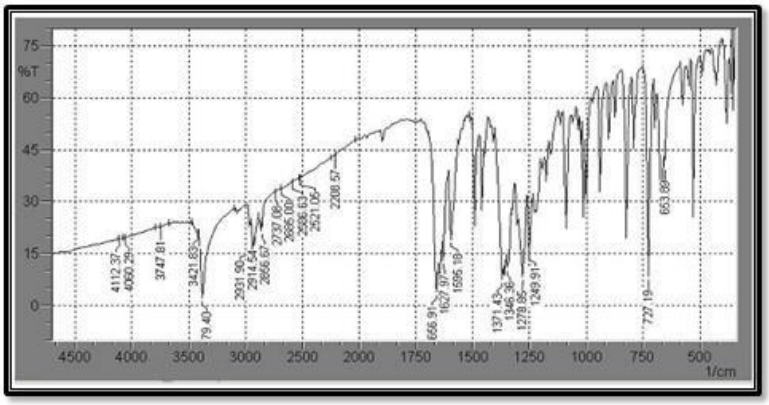

Fig. 2: FTIR spectrum of PRG.

Table 3: Principal peak and chemical group present in IR spectrum of PRG.

Functional group	-1 Reported peak(cm)	-1 Observed peak(cm)
Ar. C-H stretch	3020-2901	2931.90
C=O stretch	1800-1600	1627.97
O-H stretch	3750-3600	3747.81

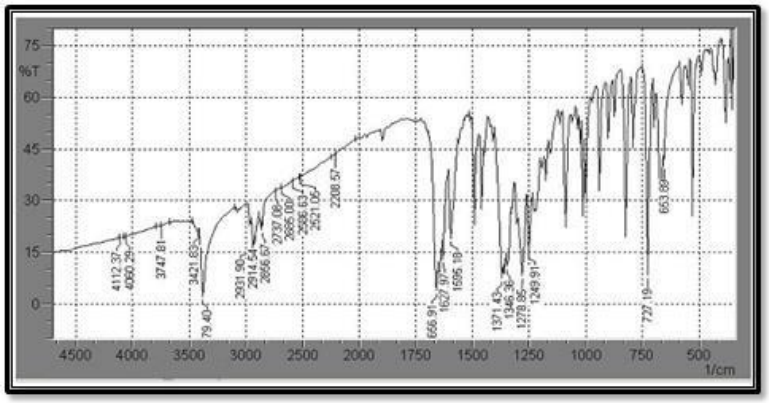

Fig. 3: Infrared spectrum of PRG.

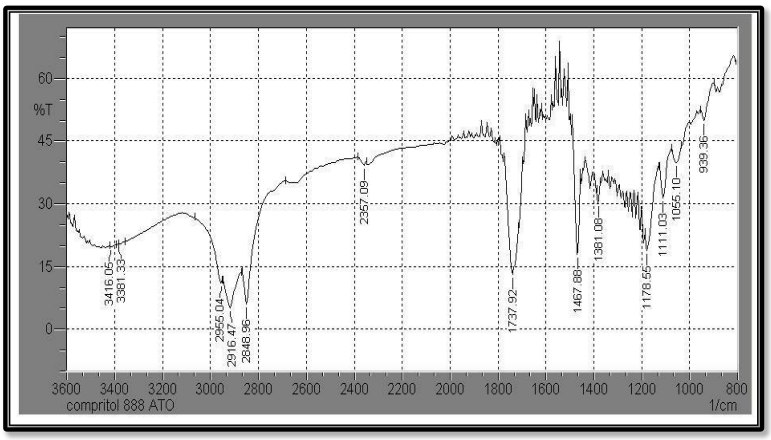

Fig. 4: Infrared spectrum of COMP.

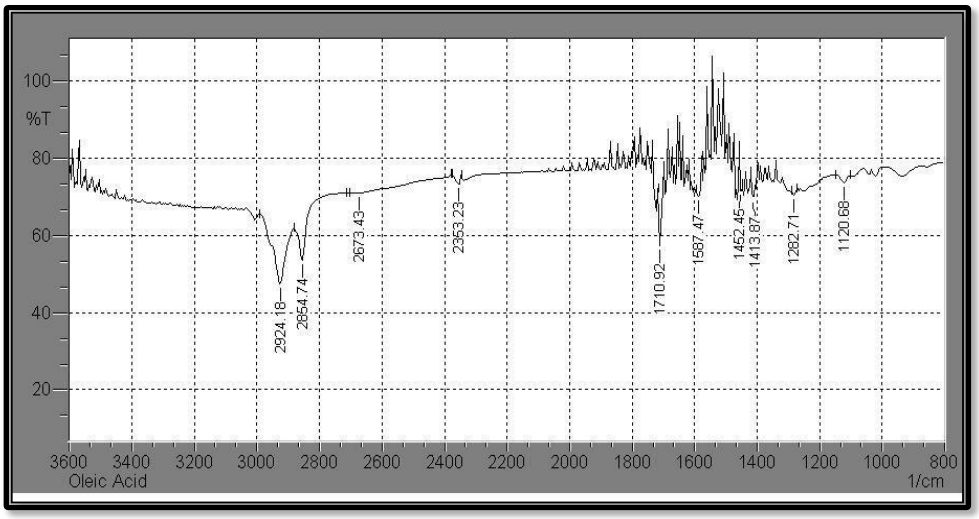

Fig. 5: Infrared spectrum of Oleic Acid.

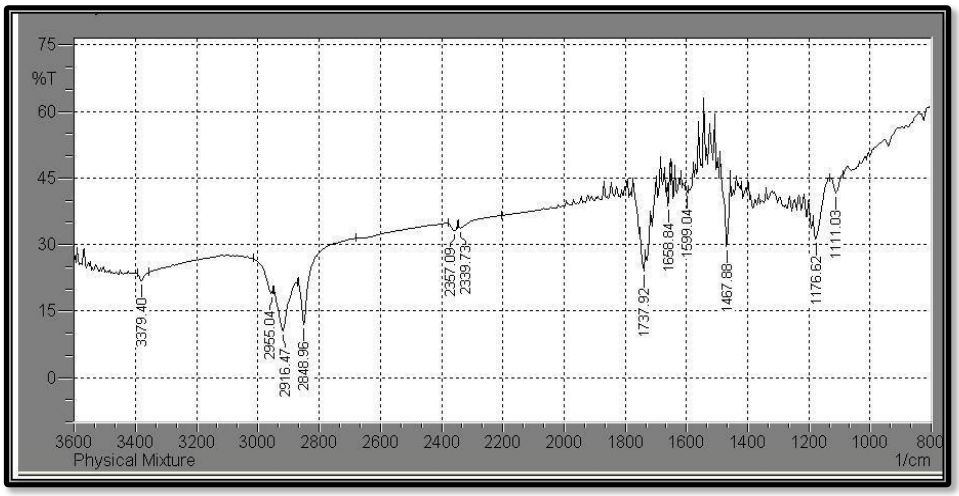

Fig. 6: Infrared spectrum of Physical Mixture.

Table 4: Drug - Excipient Interaction Studies by IR Spectroscopy.

Functional Group	Peak observed at wave number (cm^{-1})			
	PRG	COMP	OA	Physical mixture
Ar. C-H stretch	2931.90	2916.47	2924.18	2916.47
C=O Strech	1627.97	-	1710.47	1645.33
O-H Blend	3747.81	-	-	3404.47
Ar. C-Cl	727.19	-	-	-
C-C Strech	1249.91	1178.95	-	1278.13
CH_3 bend	1371.43	1467	1452.45	1425.74

Wave numbers of principle peaks of PRG were found to be present in the FTIR spectra of physical mixture. Thus, there observed no interaction between drug and polymer. Thus, it can be concluded that there have been no major effects or changes in the properties of drug which affects the stability of PRG in these mixtures and hence it is proved that formulations are stable and do not showing any significant interactions.

Differential Scanning Calorimetry Study

- The DSC thermograms were recorded for PRG, COMP and physical mixture. The DSC heating and cooling curves were recorded as plot of enthalpy in mW vs. Temperature in C.

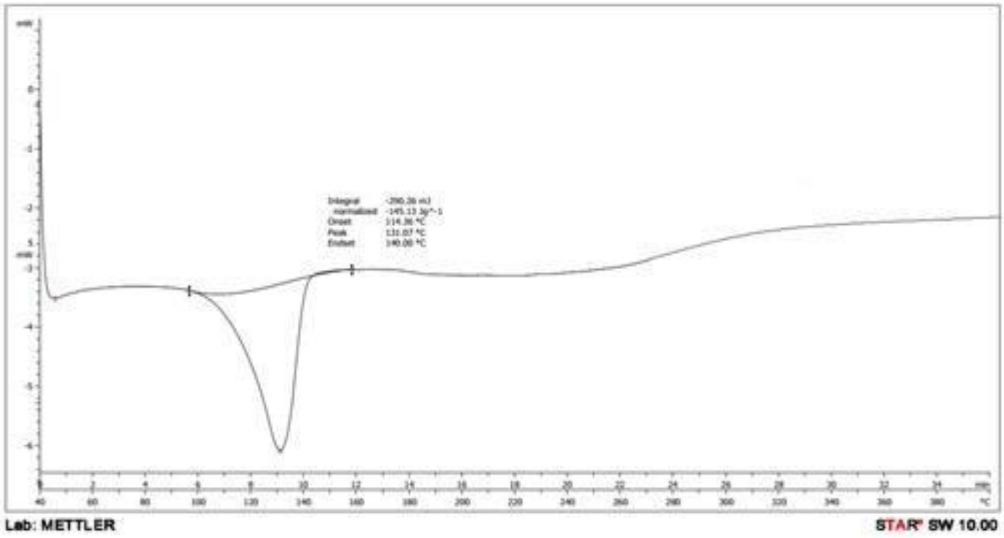

Fig. 7: DSC thermogram of pure PRG.

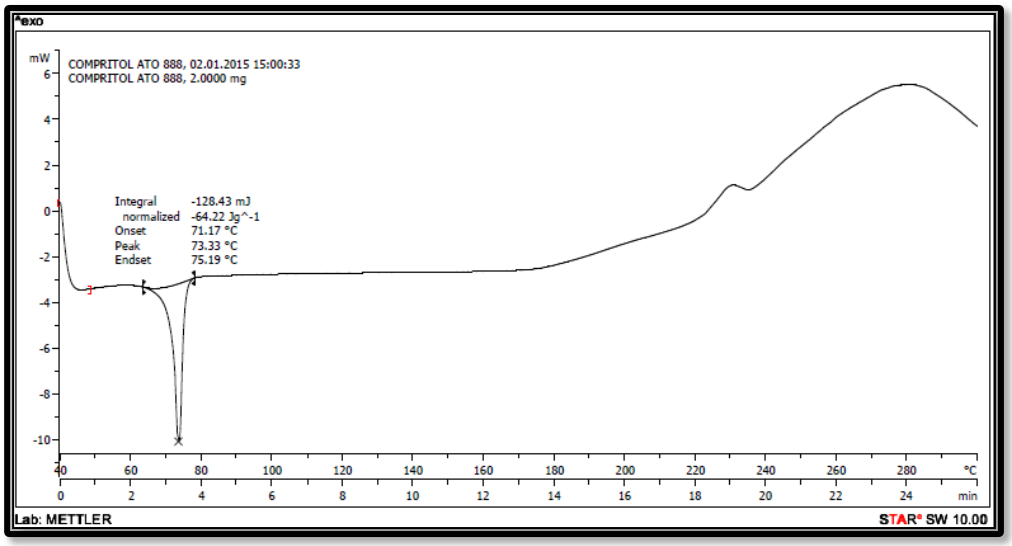

Fig. 8: DSC thermogram of COMP.

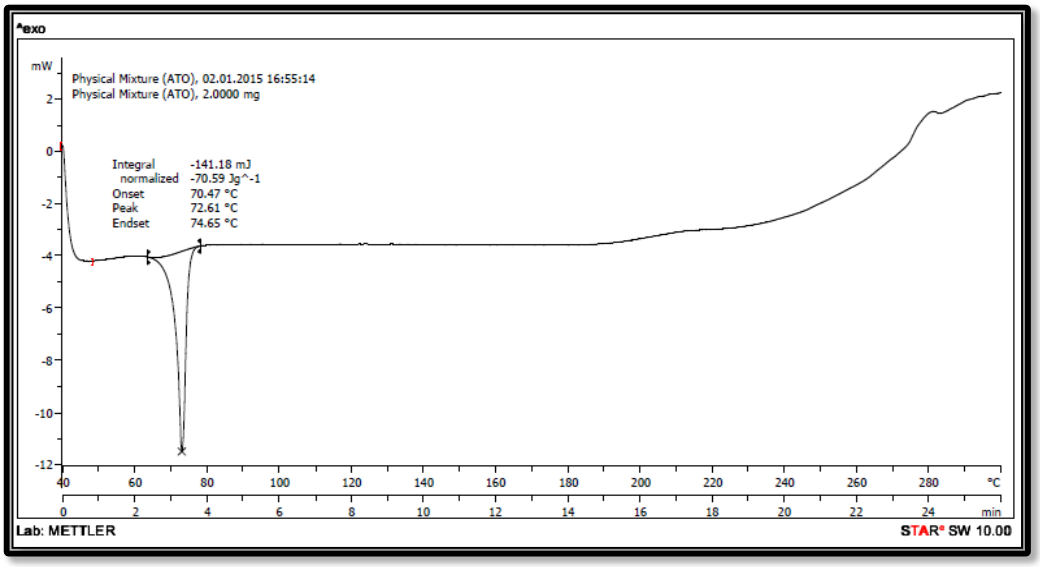

Fig. 9: DSC thermogram of physical mixture.

For PRG, the melting process took place at 220.07°C **(Fig 7)** and for bulk material of COMP melting process took place at 71.17°C **(Fig 8).** No significant change in the position of endothermic peaks was observed after running the physical mixture **(Fig 9).** Thus, physical incompatibility between the components was discarded.

STANDARD CALIBRATION CURVE

Standard calibration curve of PRG in Methanol

Graph of absorbance vs. concentration was plotted and found to be linear over the range of 3 to 18 µg/mL indicating its compliance with Beer's and Lambert's law. Results are shown in **Table 5**.

Table 5: Standard calibration curve of PRG in methanol.

Sr. no.	Conc (µg/ml)	Abs
1	3	0.16
2	6	0.322
3	9	0.459
4	12	0.611
5	15	0.758
6	18	0.909

Standard calibration curve of PRG in pH 1.2 Phosphate Buffer

Graph of absorbance vs. concentration was plotted and found to be linear over the range of 15 to 90µg/mL indicating its compliance with Beer's and Lambert's law. Results are shown in **Table 6.**

Table 6: Standard calibration curve of PRG in pH 1.2 Phosphate Buffer.

Sr. no	conc. (µg/ml)	Abs.
1	15	0.145
2	30	0.296
3	45	0.456
4	60	0.614
5	75	0.786
6	90	0.938

Standard calibration curve of PRG in pH 6.8 Phosphate Buffer

Graph of absorbance vs. concentration was plotted and found to be linear over the range of 5 to 35µg/mL indicating its compliance with Beer's and Lambert's law. Results are shown in **Table 7.**and **Fig 10.**

Table 7: Standard calibration curve of PRG in pH 6.8 Phosphate Buffer.

Sr. no	Conc (µg/ml)	Abs.
1	5	0.152
2	10	0.295
3	15	0.429
4	20	0.581
5	25	0.72
6	30	0.87
7	35	0.99

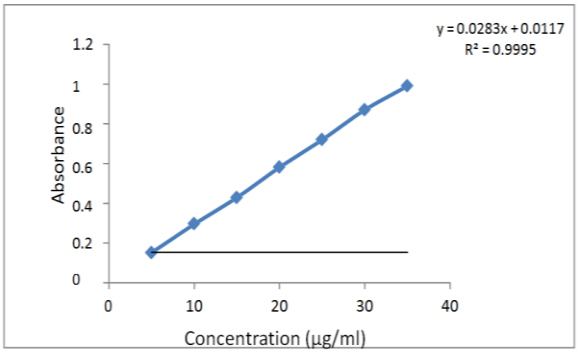

Fig. 10: Standard calibration curve of PRG in pH 6.8.

Standard calibration Curve of PRG in pH 7.4 Phosphate Buffer

Graph of absorbance vs. concentration was plotted and found to be linear over the range of 2 to 14µg/mL indicating its compliance with Beer's and Lambert's law. Results are shown in **Table8** and **Fig 11.**

Table 8: Standard calibration Curve of PRG in pH 7.4 Phosphate Buffer.

Sr. no	Conc. (µg/ml)	Abs.
1	2	0.123
2	4	0.254
3	6	0.369
4	8	0.498
5	10	0.625
6	12	0.765
7	14	0.9

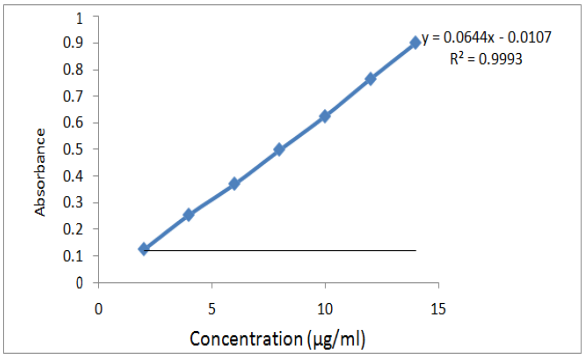

Fig 11: Standard calibration curve of PRG in pH 7.4.

FORMULATION AND DEVELOPMENT

Partitioning behavior of PRG between the Lipids

Based on the screening of liquid lipids for the maximum solubility of the drug as tabulated in **Table 9** and **Table 10** oleic acid was screened out as most suitable liquid lipid to be used in the PRG-NLCs. In case of solid lipid screening COMP emerged as most suited solid lipid for the formulation of PRG-NLCs. Moreover, both the lipids are non-toxic in nature, approved by regulPRGry status, inexpensive etc., and hence were used in the formulation.

Table 9: Solubility of PRG in different oils.

Sr. no.	Ingredients	Solubility (Conc. mcg/ml)
1	Oleic acid	24.952±0.098
2	Sunflower oil	14.672±0.1200
3	Coconut oil	19.184±0.011
4	Arachis oil	19.962±0.062
5	Castor oil	17.65±0.051
6	Seasum oil	11.948±0.119

n=3*

Table 10: Amount of PRG dissolved in 1 gm. solid lipid.

Sr. no.	Ingredients	Amount of drug dissolved in 1 gm solid lipid
1	GMS	22.941±0.1908
2	Precirol	17.935±0.1566
3	Compritol 888 PRG	28.624±0.1166
4	Stearic acid	19.845±0.400
5	Palmitic acid	21.911±0.0787
6	Carnuba wax	12.634±0.402

Preparation of PRG loaded NLCs

PRG-NLCs were prepared using hot high pressure homogenizer as it is the best, reliable and powerful technique used in the scale up production **(Muller et al, 2000; Mehnert and Mader, 2001)**. Indeed, it has been reported that lipid nanoparticles stabilized with surfactants or polymers and their mixtures (Lipoid S 75 and Poloxamer 188) have lower particle sizes and higher storage stability compared to formulations with only one surfactant **(Mehnert and Mader, 2001)**. It was observed from the preliminary sudies that 800 bars of pressure is enough to produce nanoparticles having a particle size of 200-300 nm. While the number of cycles through HPH was fixed to 5 cycles, it was seen that by inreasing the number of cycles there was a increase in the surface kinetic energy over the particles leading to aggregration of the nanoparticle causing increase in particle size. Higher stirring rates did not significantly change the particle size, but slightly improved the polydispersity index. Considering the low solubility and absorption of PRG from the GI tract, the actual amount of drug bioavailable to the body is only about 23%, because of poor solubility of PRG. For this reason, the NLCs were selected to improve the oral bioavailability of PRG, which is goes through the lymphatic absorption pathway **(Yuan et al., 2007)**. Many parameters may be involved in the process for the development of formulation of NLCs. To minimize the number of tests and in attempt to optimize the NLCs, CCRD–RSM was used for designing the least number of runs. The PRG loaded NLCs were prepared using hot HPH technique. For the preparation of PRG-NLCs, COMP was selected as a solid matrix and Oleic acid as liquid lipid respectively, as mentioned above. The homogenizer pressure was optimized to 800 bars for 5 cycles **(Zhang et al., 2013; Varshosaz et al., 2009)**.

Experimental Factorial Design and Data Analysis

The CCRD–RSM methodology offers to investigate a high number of variables at different levels with limited number of experiments. A mathematical relationship between factors and variables was generated by response surface regression analysis using Design-Expert® (version 8.0.1, Stat-Easc, Inc., Minneapolis, MN, USA) software. The 3D response surface graphs are shown in **Figure 33-36.** To fit the data, a quadratic polynomial model was chosen as the best model. Additionally, analysis of variance (ANOVA) results were calculated by this software. **Eq. (3), (4) and (5)** the mathematical model, shows the relationship between variables and response of MPS (Y_1), ZP (Y_2) and % EE (Y_3), respectively.

Table 11: Summary of results of regression analysis for responses Y_1, Y_2 and Y_3.

Models	R^2 Value	Adjusted R^2	Predicted R^2	S.D	C.V. %
Response (Y_1) Quadratic	0.8676	0.7485	0.1348	8.52	6.94
Response (Y_2) Quadratic	0.9522	0.9092	0.6134	0.81	4.38
Response (Y_3) Quadratic	0.8313	0.6795	0.3091	4.11	5.91

Regression equations for fitted Quadratic interactive model

Particle size = 109.9326 - 2.09593 * A - 0.39964 * B-1.90053 * C + 3.01375 *A * B + 3.71125 * A * C+ 16.40125 * B * C + 8.413442 * A^2 +10.14555 * B^2 + 0.299092 *C^2 **(3)**

Zeta potential = 20.52-0.062*A-0.69*B+0.57*C+1.89*A*B+1.47*A*C-0.82*B*C+1.36*A^2+1.77*B^2-0.26*C^2 ***(4)***

EE = 63.36-3.03 * A-1.18 * B+0.87 * C-3.24 * A * B + 3.83 * A * + 1.79 * B * + 0.76 * $A^2$3.92 * B^2 + 4.35 * C^2 ***(5)***

Table 12: Results of analysis of variance for particle size *(Y_1)*.

Parameters	DF*	SS*	MS*	F*	Significance *P*
Model	9	4755.84	528.43	7.28	0.0023
Residual	10	725.69	72.57	-	-
Total	19	5481.53	-	-	-

*DF indicates degrees of freedom; SS sum of square; MS mean sum of square and F is Fischer's ratio.

Table 13: Results of analysis of variance for zeta potential (Y_2).

Parameters	DF*	SS*	MS*	F*	Significance *P*
Model	9	132.02	14.67	22.14	0.0001
Residual	10	6.62	0.66	-	-
Total	19	5481.53	-	-	-

*DF indicates degrees of freedom; SS sum of square; MS mean sum of square and F is Fischer's ratio

Table 14: Results of analysis of variance for Entrapment Efficiency (EE%) (Y_3).

Parameters	DF*	SS*	MS*	F*	Significance *P*
Model	9	830.96	92.33	5.48	0.0069
Residual	10	168.59	16.86	-	-
Total	19	999.55	-	-	-

*DF indicates degrees of freedom; SS sum of square; MS mean sum of square and F is Fischer's ratio.

Effect of surfactant concentration on the particle size, EE and zeta potential Different surfactant concentrations have shown very predominant effect on the particle size of the PRG-NLCs. The particle size was found to decrease with increase in the surfactant concentration at a constant amount of lipid (i.e. inversely proportional). A higher surfactant concentration reduces the surface tension and facilitates partitioning for the duration of homogenization **(Farahani et al., 2010).** The decrease in the particle size is accompanied by a tremendous increase in the surface area. Thus, the process of primary coverage of the newer surfaces competes with the agglomeration of the uncovered surface. The presence of surfactant molecules stabilizes the formulation by forming a thick protective layer around the droplets which prevent the coalescence of the droplets. As the particle size of the NLCs is towards lower side, the absorption through Peyer's patches will be higher and thus, plasma concentration achieved will be higher. There was no significant effect seen on the PDI and zeta potential with the change in surfactant concentration.

Characterization and evaluation of PRG-NLCs dispersion

Determination of particle size and PDI of the PRG-NLCs

The major objective of using general optimal design was to determine the levels of the three factors i.e. solid lipid, liquid lipid, surfactant and co-surfactant which produce the NLCs with minimum particle size and maximum Entrapment efficiency. The particle size and polydispersity index (PDI) of the fabricated batches were in the range of 97.84 to 255.9 nm and 0.1 to 0.437 respectively showed in **Table 19**. It has been previously reported that number of particles of mean diameter around 0.3 and 1.0 nm are preferably absorbed by Payer's patches (which drains its content in to the lymphatic system) in comparison to particles of 3.0 µm **(Shakweh et al., 2005)**. As the particle size obtained in the present study is within the size range (100 to 150 nm).

Table 15: Results of analysis of variance for zeta potential (Y_2).

Parameters	DF*	SS*	MS*	F*	Significance *P*
Model	9	132.02	14.67	22.14	0.0001
Residual	10	6.62	0.66	-	-
Total	19	5481.53	-	-	-

*DF indicates degrees of freedom; SS sum of square; MS mean sum of square and F is Fischer's ratio

Table 16: Results of analysis of variance for Entrapment Efficiency (EE%) (Y_3).

Parameters	DF*	SS*	MS*	F*	Significance *P*
Model	9	830.96	92.33	5.48	0.0069
Residual	10	168.59	16.86	-	-
Total	19	999.55	-	-	-

*DF indicates degrees of freedom; SS sum of square; MS mean sum of square and F is Fischer's ratio.

Response surface plots analysis

From **Fig 7.15**, it can be concluded that the particle size goes on decreasing as the total lipid concentration (A) increases up to certain level afterward particle size increases and similar liquid lipid concentration (B) effect was observed and **Fig 7.16**, can conclude that particle size goes on decreasing as the soya lecithin concentration increases. It is summarized that total lipid concentration (A), liquid lipid to total lipid concentration (B) and soya lecithin (C) concentration has significant effect on the particle size. Particle size gets decreases with the decrease in total lipid concentration and increases liquid lipid concentration and soya lecithin concentration. From **Fig 7.17**, it can be conclude that the zeta potential goes on increasing as total lipid concentration get decreased and liquid lipid to total lipid concentration get increased. **Fig 7.18** can conclude that zeta potential goes on decreased as liquid lipid to total lipid concentration and soya lecithin concentration get increased. From **Fig 7.19**, it can be concluded that the EE goes on increasing as the total lipid concentration (A) increases and liquid lipid to total lipid concentration increases and **Fig 7.20**, can conclude that EE goes on increasing as the liquid lipid concentration (B) increases and soya lecithin concentration (C) decreases i.e. with the increase in lipid.

Table 16: Results of analysis of variance for zeta potential (Y_2).

Parameters	DF*	SS*	MS*	F*	Significance *P*
Model	9	132.02	14.67	22.14	0.0001
Residual	10	6.62	0.66	-	-
Total	19	5481.53	-	-	-

*DF indicates degrees of freedom; SS sum of square; MS mean sum of square and F is Fischer's ratio

Table 17: Results of analysis of variance for Entrapment Efficiency (EE%) (Y_3).

Parameters	DF*	SS*	MS*	F*	Significance *P*
Model	9	830.96	92.33	5.48	0.0069
Residual	10	168.59	16.86	-	-
Total	19	999.55	-	-	-

*DF indicates degrees of freedom; SS sum of square; MS mean sum of square and F is Fischer's ratio.

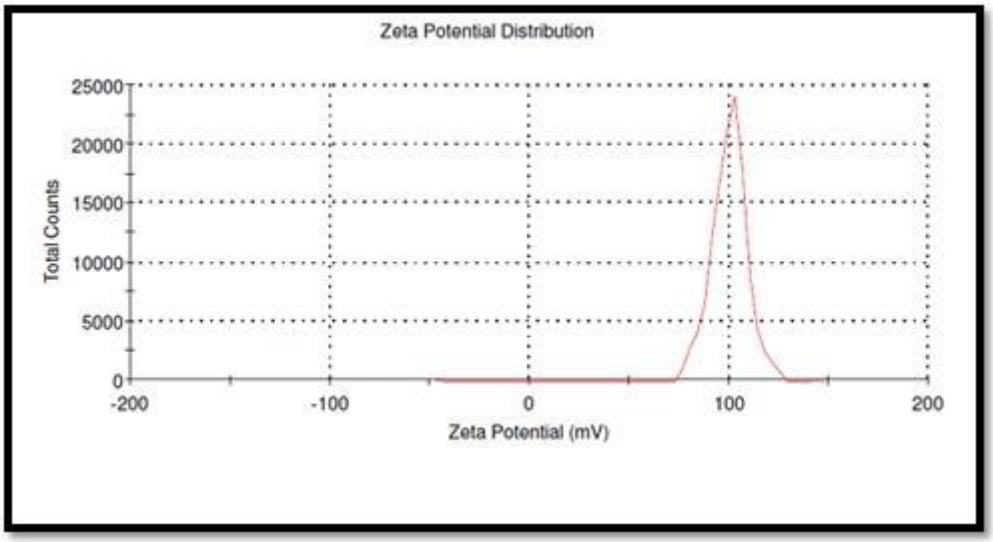

Fig. 11: Zeta potential analysis of Optimised batch (F8).

Determination of entrapment efficiency (EE %) and loading efficiency (LE %) of the PRG-NLCs

The EE is mainly dependent on the nature of the drug and the lipidic phase in which the drug is encapsulated. As the PRG is a lipophilic drug and its solubility is also greater in the COMP (conclusion drawn from partition coefficient study), the EE apparently was found to be higher, i.e. in the range of 54.83- 82.58%). The LE was found to be in the range of 3.87–13.74%.

***In vitro* release studies of PRG-NLCs**

In vitro drug release study of the PRG loaded NLCs optimised batch (F8) showed the sustained release behaviour in 6.8 pH phosphate buffer. The cumulative percentage release of PRG from PRG-NLCs was investigated *in vitro* over a period of 96 h. Each sample was analyzed in triplicate and release curves are shown in **Fig 12.** It was indicated that NLCs released almost 97.27 % of the drug at the end of 96 h. The increase in lipid concentration had significant effect on the PRG release which prolonged the release of the PRG from NLCs **(Agrawal et al., 2010).** It may be due to the equal distribution of drug within the lipid matrix and good entrapment of PRG in COMP.

Table 18: In vitro drug release profile (optimized batch F8) of PRG-NLCs (n=3, mean ± SD).

Time (h)	% CDR
0	0
1	7.111 ± 1.75
3	13.027 ± 1.98
6	24.229 ± 2.21
12	34.017 ± 2.12
24	41.713 ± 1.91
36	51.802 ± 1.58
48	60.739 ± 1.32
60	73.86 ± 1.57
72	83.79 ± 1.85
84	91.976 ± 2.14
96	97.27 ± 1.95

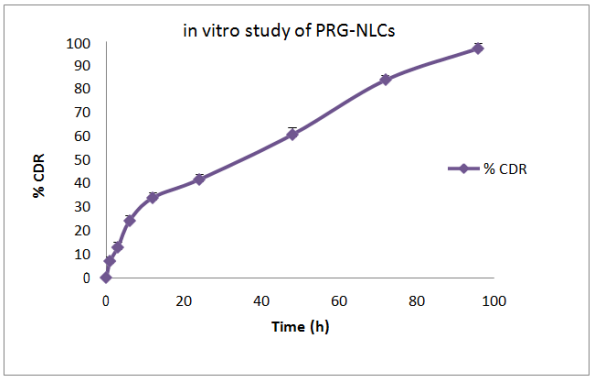

Fig 12: *In vitro* drug release profile (optimized batch F8) of PRG-NLCs (n=3, mean ± SD).

Kinetic model fitting of optimized PRG – NLCs

Batch Code	Zero order (R^2)	First order (R^2)	Higuchi (R^2)	Korsmeyer-Peppas		Best fitted model	Order of release	Release Mechanism
				(R^2)	n			
F8	0.967	0.333	0.928	0.261	0.41	Zero order	Fickian	Diffusion

SOLID STATE CHARACTERIZATIONS

Lyophilization of PRG – NLCs

The lipid dispersion was successfully freeze dried using the benchtop freeze dryer. Lyophilisation was carried out for optimised batch at -75°C with 3% mannitol as a cryoprotectant. The role of cryoprotectant is to decrease nanoparticle aggregation during the process of freeze-drying. The obtained lyophilised powder was found to be dry, porous and friable after 72 h. The vacuum was maintained at 76 mTorr.

Scanning electron microscopy (SEM)

Morphological study of optimum formulation was done by taking SEM pictures of prepared NLCs. It was revealed that they were uniformly distributed **(Figure 13).** Studies also verified that the crystalline PRG is converted to its amorphous form as it was encapsulated by lipids. Studies showed that the predicted particle size and measured size with a zetasizer was comparable with size of particles that were observed by SEM.

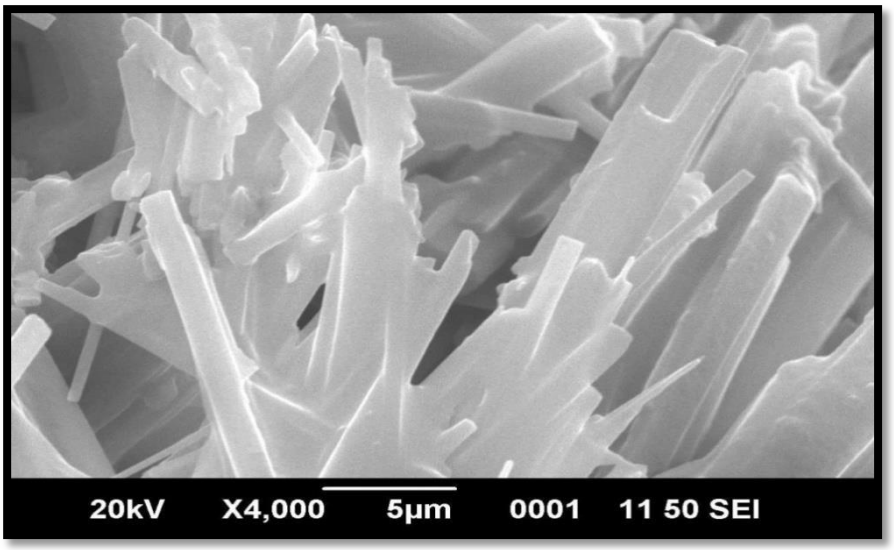

Fig. 13: Scanning electron microscopy of optimized PRG-NLC.

X-Ray Diffraction (XRD)

X-ray diffraction patterns of pure crystalline drug (A), physical mixture of drug and COMP (B), and drug-loaded lyophilized NLC formulation (C) shown in **Fig 14**. The typical crystalline nature of drug was defined by observing sharp principal peaks of PRG between 7 to 47 on 2θ scales. The 2θ scattered angle of drug was found to be 18.88º, 19.53º, 23.06º, 26.62º (A). Distinctive sharp peaks of drug were disappeared in drug loaded freeze dried NLC formulation (C). The scale of formulation was found to be 17.57º, 21.60º, 20.68º, 20.11º although both broad peak and sharp peak were obtained in physical

mixture of drug and COMP (B). These results were in good support with DSC results, indicating the PRG conversion of crystalline to amorphous state.

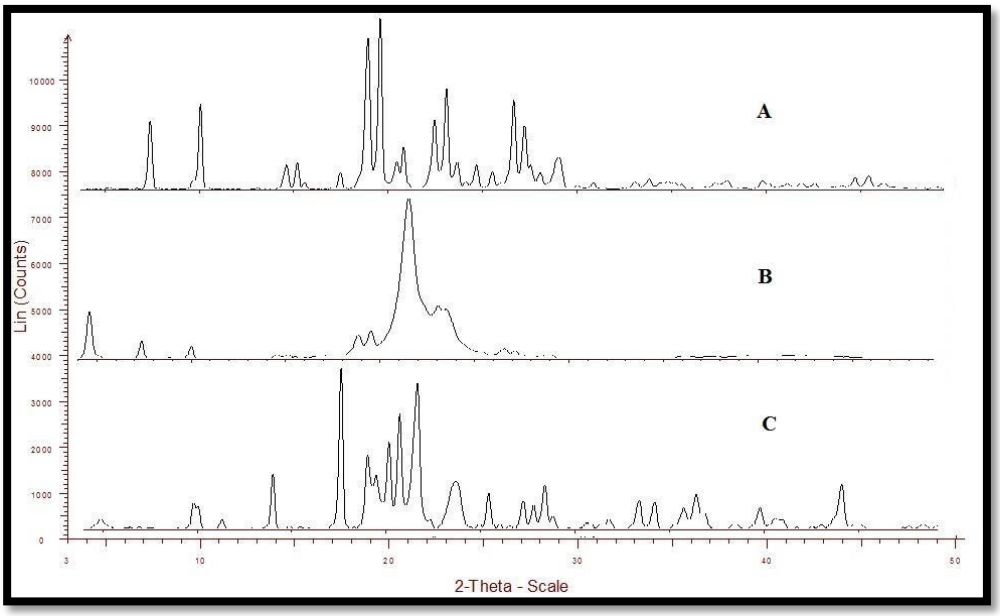

Figure 14: XRD pattern of A) pure drug, B) physical mixture of drug and COMP, and C) drug-loaded lyophilized NLC formulation.

Accelerated stability studies

Accelerated stability studies were conducted on optimised NLCs (F8) using the particle size, PDI and EE as the prime parameters. There was a slight increase in the particle size during the three months storage from the 108.97 ± 04 nm to 135 ± 05 nm with not much change in PDI (i.e. initially which was 0.237 ± 0.10 and that after 3 months it was 0.252± 0.23. The EE (%) of the optimised batch initially was found to be 82.58 ± 3.2 % while that after 3 months was found to be 79.17 ± 4.7% indicating that the drug can retain within the nanoparticles for the sufficient period of time. On storage of the NLCs (F8), there were no significant alterations in the size, PDI and EE % of the NLCs. Hence, they were found to be stable at 25 ± 2 ºC/60 ± 5% RH for a total period of 3 months.

Table 19: Stability characteristics of PRG-NLCs formulation in terms of mean particle size, polydispersity index (PDI) and entrapment efficiency.

Stability Parameter	Test period			
	0 month	1 month	2 month	3 month
Particle Size (nm)	108.97 ± 04	115.25 ± 05	127.14 ± 03	135 ± 05
PDI	0.237 ± 0.10	0.242 ± 0.14	0.244 ± 0.11	0.252 ± 0.10
% EE	82.58 ± 3.2	78.42 ± 2.12	73.05 ± 3.4	69.17 ± 4.1

SUMMARY AND CONCLUSION

Summary

Solubility of a drug is an important property that mainly influences the extent of oral bioavailability. Enhancement of oral bioavailability of poorly water soluble drugs is the most challenging aspects of drug development. It is very important to find appropriate formulation approaches to improve the aqueous solubility and bioavailability of poorly aqueous soluble drugs.

PRG, chemically, (1-[amino-(4-chloroanilino)methylidene]-2-propan-2-ylguanidine, it has a potential therapeutic activity against *Toxoplasmosis gonadii, P. falciparum malaria, Pneumonia carinii, babesia and Leishmania*. It is practically insoluble in water and poorly absorbed from the gastrointestinal (GIT). Therefore, it is very important to introduce effective methods to enhance the solubility and dissolution rate of drug, substantially leading to its bioavailability.

PRG belongs to Biopharmaceutical Classification System (BCS) class II drug and exhibits mean bioavailability 23% due to its poor aqueous solubility, Therefore, its bioavailability must be enhanced via lymphatic transport system by incorporating into NLCs. NLCs are the novel generation of lipid NPs, generated to overcome the drawbacks of SLNs. Due to several imperfections in NLCs, drug-loading capacity is enhanced and drug expulsion during storage is minimized at a greater extent as compared to SLNs.

PRG-NLCs were formulated by hot high pressure homogenization (HPH) technique after lipid screening by using central composite design the three factors: Total lipid concentration, liquid lipid to total lipid concentration and co-surfactant concentration. optimizing the formula by observing the effect on three variables: mean particle size (MPS), zeta potential (mV) and percentage entrapment efficiency (% EE). Thus there three variables act as dependent variables (response variables). In the present study, the role of NLCs was observed to improve oral bioavailability of PRG. COMP and Oleic acids was selected as solid lipid and liquid lipid to encapsulate PRG. Total 20 batches were suggested by software, out of which 5 batches were repeated, so total 15 batches of PRG-NLCs were formulated. The MPS and ZP of the designed batches of PRG-NLCs were in the range from 97.84 – 255.9 nm and −23.2. to −11.7 mV, respectively. The % EE was observed in the range from 54.83 - 82.58 % means can be said that prepared NLCs have good % EE. Best optimized batch (F8) was selected on the basis of MPS and% EE. The *in vitro* drug release study was performed via dialysis bag diffusion study by using phosphate buffer 6.8 as a dissolution medium of the optimized batch and found satisfactorily. The cumulative % drug release with respect to time of optimized PRG- NLCs was found to be 97.27%. Further, physicochemical characterization of PRG loaded NLCs was done by examining the results of scanning electron microscopy, differential scanning calorimetry, X-ray diffraction pattern. The *in vivo study* of PRG-NLCs was examined by the pharmacokinetic parameters were investigated by plasma analysis of male Wistar Albino rats. The stability study was performed of the optimized batch according to International Conference on Harmonisation (ICH) Q1A (R2) guidelines. It was determined that bioavailability of PRG-NLCs was 2.231 fold higher than PRG suspension. Therefore, it became evident that bioavailability can be enhanced by entrapping PRG to NLCs. The microscopic study indicated smooth surface, rod shape and uniform size distribution. From stability study of the lyophilized formulation it was found that the particle size and % EE was not changed significantly. NLCs were found to be stable for the period of 3 months at 25 ± 2°C and 60 ± 5% RH.

CONCLUSION

In this drug delivery system, PRG was successfully incorporated into NLCs by hot HPH method with high entrapment efficiency due to its high lipophilicity. Compared with other methods, main advantage associated with it, there is no need to use any organic solvent. The PRG-NLCs were formulated using central composite design and response surface methodology by fitting quadratic model to the response data. An optimized formulation was selected by MPS analysis and % EE. The prepared NLCs were found to have an amorphous structure and rod shape morphology. The *in vitro* release pattern showed a sustained and continuous release of PRG-NLCs. By The *in vivo* pharmacokinetic studies revealed prolonged Tmax and improved oral bioavailability (more than 2.231 fold) via oral administration in rats. Thus, NLCs can be demonstrated as a potential carrier to improve oral bioavailability of PRG based on our experimental results with higher entrapment efficiency.

REFERENCES

1. Abdelwahed, W., Degobert, G., Stainmesse, S., Fessi, H. Freeze-drying of nanoparticles: Formulation. Process and storage considerations. *Adv. Drug Delivery Rev.*, 2006; 58: 1688- 13.
2. Agrawal, Y., Petkar, K., Sawant, K. Development, evaluation and clinical studies of Acitretin loaded anostructured lipid carriers for topical treatment of psoriasis. *Int. J. Pharm.*, 2010; 401: 93-102.
3. Alex, M. R. A., Chacko, A. J., Jose, S. and Souto, E. B. Lopinavir loaded solid lipid nanoparticles (SLN) for intestinal lymphatic targeting. *Eur. J. Pharm. Sci*., 2011; 42: 11–18.
4. Araujo, J., Mira, EG., Egea, MA., Garcia, ML., Souto, EB. Optimization and physicochemical characterization of a triamcinolone acetonide-loaded NLC for ocular antiangiogenic applications. *Int. J. Pharm*., 2010; 393: 167-175.
5. Avgoustakis, K., Beletsi, A., Panagi, Z., Klepetsanis, P. Effect of copolymer composition on the physicochemical charcteristics in vitro stability and biodistribution of PLGA- m PEG nanoparticles. *Int. J. Pharma.*, 2003; 259: 115-127.
6. Baggish, AL and Hill, DR. Antiparasitic Agent Atovaquone, *Antimicrob. Agents Chemother*, 2002; 1163–1173.
7. Bangham, A. D. Liposomes: realizing their promise. *Hosp. Pract.*, 1992; 27(12): 51- 61.
8. Barratt, G. Therapeutic applications of colloidal drug carriers. *Pharm. Sci. Technol. Today*, 2000; 3(5): 163-71.
9. Blasi, P., Giovagnoli, S., Schoubben, A., Ricci, M., Rossi, C. Solid lipid nanoparticles for targeted brain drug delivery. *Adv. Drug Deliv. Rev*., 2007; 59: 454–477.
10. Box, G., Wilson, K. on the experimental attainment of optimum conditions, Journal of the Royal Statistical Society. *Series B Statistical Methodology*, 1951; 13: 1– 45.
11. Calvo, J., Lavandera, J., Agueros, M., Irache, J. Cyclodextrin/poly (anhydride) nanoparticles as drug carriers for the oral delivery of atovaquone. *Biomed microdevices*, 2011; 13: 1015-1025.
12. Cauchetier, E., Deniau, M., Fessi, H., Fessi A, Paul M. Atovaquone-loaded nanocapsules: influence of the nature of the polymer on their in vitro characteristics, *Int J Pharm.*, 2003; 250: 273- 281.
13. Cavalli, R., Marengo, E., Rodriguez, L., Gasco, MR. Effects of some experimental factors on the production process of solid lipid nanoparticles. *Eur. J. Pharm.* and *Biopharm*, 1996; 43: 110-115.
14. Chakraborty, S., Shukla, D., Mishra, B., Singh, S. Lipid – An emerging platform for oral delivery of

drugs with poor bioavailability. *Eur J Pharm and Biopharm*, 2009; 73: 1–15.
15. Chowdary, KP., Rao, SA. Nanoparticles as drug carriers. *Indian drugs*, 1997; 34: 549-53.
16. Dalencon, F., Amjaud, Y., Lafforgue, C., Derouin, F., Fessi, H. Atovaquone and rifabutine-loaded nanocapsules: formulation Studies, *Int. J. Pharm*., 1997; 153: 127–130.
17. Das, ST., Chaudhury, A. Recent advances in lipid nanoparticle formulations with solid matrix for oral drug delivery. *AAPS Pharm. Sci. Tech*., 2011; 12: 62-76.
18. Driscall, MC. Lipid based formulation for intestinal lymphatic delivery, *Euro. J. pharma. Sci.*, 2002; 15: 405-415.
19. Egbaria, K. Weiner, N. Liposomes as a topical drug delivery system. *Adv. Drug Delivery Rev*., 1990; 5: 287-300.
20. Ekambaram, P., Sathali, A., Priyanka K. Solid Lipid Nanoparticles: a Review *Sci. Revs. Chem. Commun*, 2012; 2: 80-102.
21. European pharmacopoeia, 2004; 5th edition, 1178-79.
22. F.J. Araujo, J. Huskinson, J.S. Remington, Antimicrob. Agents *Chemother*, 35.
23. Fang, J., Fang, C., Liu, C., Su, Y. Lipid nanoparticles as vehicles for topical psoralen delivery: Solid lipid nanoparticles (SLN) versus nanostructured lipid carriers (NLC). *Eur J Pharm and Biopharm*, 2008; 70: 633–640.